A model for the control of multileaf collimator and related inverse planning algorithm

J. Tervo, P. Kolmonen

Report A/1999/5

ISBN 951-781-613-8
ISSN 0787-6416

UNIVERSITY OF KUOPIO

Department of Computer Science and Applied Mathematics

P.O.Box 1627, FIN-70211 Kuopio, FINLAND

A model for the control of multileaf collimator and related inverse planning algorithm

J. Tervo
Department of Computer Science and Applied Mathematics,
University of Kuopio
Research Institute for Radiotherapy Research,
Department of Applied Physics,
University of Kuopio

P. Kolmonen
Research Institute for Radiotherapy Research,
Department of Applied Physics,
University of Kuopio

Abstract

A new approach for the inverse treatment planning in radiation therapy with the multileaf collimator (MLC) technique is presented. The application of the MLC-techniques requires an algorithm for the computation of the positions or velocities of leaves as a function of time such that the prescribed dose in the patient space is obtained. First the intensity distribution in the treatment space is determined applying some inverse treatment techniques. Then an MLC control algorithm which generates the determined intensity distribution is required. In the present paper a mathematical model is given which controls the MLC such that the intensity distribution is obtained under selected dose constraints. In addition an MLC control algorithm not requiring an intensity distribution as an intermediate step is expressed. The algorithm uses the MLC leaf positions and delivery times directly in inverse treatment planning. The method can easily be implemented to multiple static treatments ("step-and-shoot") but a modification to dynamical MLC techniques is also straightforward.

AMS-classification: 49-04, 92C50, 93-04

1 Introduction

Conformal radiation treatment planning with MLC traditionally faces with two inverse problems. The first one is to determine the intensity distribution in the treatment space in such a way that the prescribed dose distribution in the patient space is obtained. The second problem is to determine the trajectories of the leaves of the multileaf collimator to produce the required intensity distribution.

For the first problem many algorithms for inverse treatment planning have been developed (e.g. [3, 4, 5, 8, 6, 9, 11, 12, 15, 19, 25, 27]). As to the second problem the methods to control the collimator leaves can be divided into two cathegories: (1) In dynamic MLC techniques the leaves can be moved during the treatment delivery and so the dose is delivered continuously corresponding to each individual field. The radiation is interrupted during the selection of subsequent fields. For the implementation of this method one has applied e.g. so called "closed in" and "sweep up" techniques [14, 16, 17]. (2) In the multiple static collimation techniques the positions of the leaves are discretely changed between subfields. The irradiation is interrupted during the motion of the leaves [1, 20, 22, 28].

One of the advantages in the use of multiple static techniques is the easier control of leaves since the limited velocity and acceleration of leaves are not needed to take into account. In the dynamic collimation

the maximal velocity (and acceleration) will be one of the constraints in optimization algorithms. A disadvantage of the multiple static collimation is that it may prolong the whole treatment time.

Our aim is to express an algorithm for the control of the multileaf collimation which is based on the use of an explicit object function. This enables an easy application of the physical limitations of the multileaves. The second advantage of our algorithm is that this approach makes it possible to state the whole inverse treatment planning optimization with the help of multileaf parameters unnecessiating the determination of intensity distribution as an intermediate step. This idea is based on the following observation.

Applying the pencil beam model dose $D(x)$ in the patient space V can be given by the integral

$$D(x) = \sum_{l=1}^{L} \int_U h_l(x,u)\Psi_l(u)\mathrm{d}u,\ x \in V \tag{1}$$

where the kernel $h_l(x,u)$ is a dose deposition kernel corresponding to the l^{th} field S_l and Ψ_l is the intensity distribution per unit area of S_l in the treatment space U [9]. If we assume N leaf pairs then the intensities $\Psi_{li}(u)$ in strips $U_i = [-a,a]\times]u_{2,i-1}, u_{2,i}[\subset U$ corresponding to the field S_l can be obtained by

$$\Psi_{li}(u) = \Psi_0 \int_0^{T_l} H(a_{li}(t) - u_1)H(u_1 - b_{li}(t))\mathrm{d}t,\ u \in U_i \tag{2}$$

where $a_{li}(t)$ and $b_{li}(t)$ are the leaf trajectories corresponding to the strips U_i (figure 1). Ψ_0 is the (uniform) intensity distribution per unit time and area incident on the MLC. H is the Heaviside function. The idea to use the integrals of the Heaviside function in the determination of Ψ_{li} in a certain special case originated in [1]. Combining (1) and (2) we obtain

$$D(x) = \Psi_0 \sum_{l=1}^{L}\sum_{i=1}^{N} \int_{U_i}\int_0^{T_l} h_l(x,u)H(a_{li}(t) - u_1)H(u_1 - b_{li}(t))\mathrm{d}t\mathrm{d}u,\ x \in V. \tag{3}$$

Thus the dose can be obtained with the help of leaf trajectories. Various discrete approximations lead to the practical implementation of this idea and it is demonstrated below.

In the present investigation our main interest lies in the multiple static treatment. The method is however applicable also for the dynamic treatment schemes although no practical implementation for the dynamic collimation, that is, techniques similar to "closed in" ("curtain shutter") or "sweep up" ("shrinking field") techniques is given here.

The considered inverse treatment planning algorithms lead to the large dimensional nonlinear multiextremal optimization problems. Hence a careful initialization of the problem (section 6) or an application of some global optimization scheme ([13, 7]) is needed. After the initialization we seek the feasible solution by applying the linearization of the dose function and the Cimmino algorithm ([3, 4, 9]).

2 Mathematical model for the leaf control to generate a given intensity

At first we suppose that the intensity distribution Ψ for the treatment is given. We construct a model for the control of MLC leaves such that their movements will generate the prescribed intensity. It sufficies to consider one field, say S, only.

We use the formalism of [20]. Assume that the collimator plane (treatment head) is a rectangular $U = [-a,a]\times[-b,b] \subset \mathbb{R}^2$. Denote the point of U by $u = (u_1, u_2)$. The collimator leaves are orthogonal to u_2-axis. Suppose that the leaves have a positive width d and that there are N leaf pairs (B_i, A_i), $i = 1,...,N$. This means that $2b = Nd$. Let $U_i := [-a,a]\times]u_{2,i-1}, u_{2,i}[$, $i = 1,...,N$ be the strips along u_1-axis determined by the leaf pairs (B_i, A_i) (see figure 1).

Furthermore, let $\Psi = \Psi(u) = \Psi(u_1, u_2)$ be the prescribed intensity distribution per unit area of the considered field S. We assume that Ψ is a piecewise continuous function $U \mapsto \mathbb{R}$ such that $\Psi(u)$ is

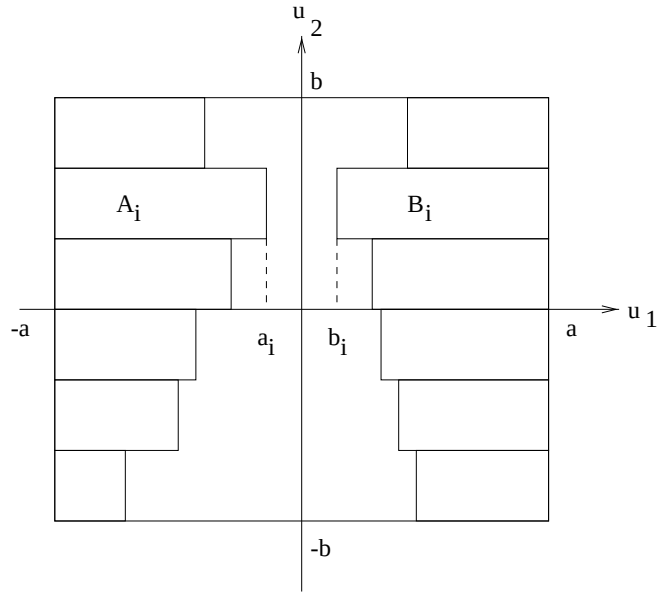

Figure 1: The geometrical setting of the treatment head. The number of leaf pairs is $N = 8$. A_i is the right hand leaf and B_i is the left hand leaf.

constant $\Psi_i(u_1)$ for $u_2 \in]u_{2,i-1}, u_{2,i}[$, that is $\Psi(u) = \Psi_i(u_1)$, for $u \in U_i$. This will be the case when we in the calculation of intensities subdivide the treatment space into bixels in such a way that the partition points in u_2- direction are exactly the points $u_{2,i}$. Let Ψ_0 be the (uniform) intensity distribution per unit time and unit area incident on the MLC. Finally, let T be the treatment time corresponding to S and let the right (left) hand head of the leaf A_i (B_i) be in a point $a_i(t) \in [-a, a]$ ($b_i(t) \in [-a, a]$) at the moment $t \in [0, T]$.

In [20] we derived that, in the case when the intensity is given, the leaf control problem for MLC can be stated as follows:

Suppose that Ψ is given. Let T be a positive number. For any $i = 1, ..., N$ determine the leaf trajectories $a_i : [0, T] \mapsto \mathbb{R}$, $b_i : [0, T] \mapsto \mathbb{R}$ such that

$$\Psi_0 \int_0^T H(a_i(t) - u_1) H(u_1 - b_i(t)) \mathrm{d}t = \Psi_i(u_1), \ u \in U_i \tag{4}$$

$$b_i(t) \leq a_i(t), \ t \in [0, T] \tag{5}$$

$$b_i(t) \geq -a, \ a_i(t) \leq a, \ t \in [0, T] \tag{6}$$

where H is the Heaviside function

$$H(x) = \begin{cases} 1, & x \geq 0 \\ 0, & x < 0 \end{cases}$$

Remark 1 *A. The above model assumes that the leaves do not produce scattered radiation and there is no leakage through or between the leaves. In practice there exist scattering and leakage in the leaves and the Heaviside function must be replaced with a modified (steplike) function. These effects are possible to take into account in the modelling. We shall consider this issue later.*

B. In the above problems besides to determine the trajectories the minimization of the treatment time T is important.

C. The Heaviside function H satisfies

$$H(x_1 - x) H(x - x_2) = H(x_1 - x) - H(x_2 - x)$$

for $x_1 > x_2$. Hence we are able to replace (4) by

$$\Psi_0 \int_0^T [H(a_i(t) - u_1) - H(b_i(t) - u_1)]\mathrm{d}t = \Psi_i(u_1),\ u \in U_i.$$

The substitution may simplify some computations. This note is (approximately) also concerning for the below done replacements of H.

3 Optimization of the leaf movements to generate a given intensity

3.1 Optimal solution for one leaf pair

For clearity we first investigate one particular leaf pair (B_i, A_i). The exact Heaviside function over the interval $[-a, a]$ is given in section 2. We replace the Heaviside function with a linear combination

$$\tilde{H}(x) = \sum_{j=1}^{r} d_j \psi_j(x) \tag{7}$$

or with the functions like

$$\tilde{H}(x) = C_1 + C_2 \overline{\mathrm{arc}}\tan(C_3 x) \tag{8}$$

$$\tilde{H}(x) = C_1 + C_2(1 - \tanh(C_3 x)) \tag{9}$$

$$\tilde{H}(x) = \mathrm{erf}_\tau(x) = \frac{1}{\sqrt{\pi}\tau} \int_{-\infty}^{x} e^{-s^2/\tau^2}\mathrm{d}s. \tag{10}$$

$\tilde{H}$ will modify the Heaviside function to achieve more realistic intensity distribution from the leaf head. In the above replacement (7) $\{\psi_j |\ j = 1, ..., r\}$ is a chosen base and d_j respective coefficients. The unknown parameters $d_j,\ C_1,\ C_2,\ C_3,\ \tau$ for (7-10) can be obtained by desirable interpolation techniques by using e.g. the measured or Monte Carlo data taking into account the scattering and leakage.

The replacement of Heaviside function with a smooth function is necessary because of head scatter and leakage. The above correction still neglects the scattering from the leaf sides and it neglects the leakage between the leaves. In addition the "groove and tongue effect" is neglected. Although we have partly considered these corrections ([20]) we omit them for simplicity. The corrections are not essential here.

For the second we assume that the leaf trajectories can be expressed by the linear combinations

$$a_i(t) = \sum_{k=1}^{n} a_{ik}\phi_k(t), \tag{11}$$

$$b_i(t) = \sum_{k=1}^{n} b_{ik}\phi_k(t) \tag{12}$$

where $\{\phi_1, ..., \phi_n\} \subset C_{\mathrm{pc}}([0, T])$ is an appropriate basis system. Here $C_{\mathrm{pc}}([0, T])$ denotes the space of piecewise continuous functions $f : [0, T] \mapsto \mathbb{R}$. In sections 3.3 and 5.3 we consider examples of the choices of basis $\{\phi_k | k = 1, ..., n\}$ and $\{\psi_j | j = 1, ..., r\}$. Since we consider a fixed (say i^{th}) leaf we can write $a_{ik} = a_k,\ b_{ik} = b_k$ without any confusion.

When we replace H by $\tilde{H}$ and substitute the expressions (11-12) to the integral (4) we obtain

$$\int_0^T Q(u_1, t)\mathrm{d}t = \Psi_i(u_1) \tag{13}$$

for $u \in U_i = [-a,a]\times]u_{2,i-1}, u_{2,i}[$ where

$$Q(u_1,t) = \Psi_0 \tilde{H}\left(\sum_{k=1}^{n} a_k\phi_k(t) - u_1\right)\tilde{H}\left(u_1 - \sum_{k=1}^{n} b_k\phi_k(t)\right). \tag{14}$$

Denote

$$\overline{a} = (a_1,...,a_n),\ \overline{b} = (b_1,...,b_n).$$

Furthermore, denote

$$q(\overline{a},\overline{b})(u_1) = \int_0^T Q(u_1,t)\mathrm{d}t. \tag{15}$$

Then by (13)

$$\Psi_i(u_1) = q(\overline{a},\overline{b})(u_1). \tag{16}$$

Our idea is based on the minimization of the norm

$$||q(\overline{a},\overline{b})(\cdot) - \Psi_i|| \tag{17}$$

with respect to $(\overline{a},\overline{b}) \in \mathbb{R}^{2n}$. Here the norm $||\cdot||$ may be e.g. the Lebesgue square norm $||f||_{L_2([-a,a])} = \left(\int_{-a}^{a}|f(u_1)|^2\mathrm{d}u_1\right)^{\frac{1}{2}}$. The norm in (17) can also be replaced with some of its discrete counterpart e.g. with the discrete square norm $||\cdot||_2$.

As a conclusion we find that the object function is defined by $f_i(\overline{a},\overline{b}) = ||q(\overline{a},\overline{b}) - \Psi_i||$. The optimization problem can be stated as follows:
Find the (global) minimum

$$\min_{(\overline{a},\overline{b})\in\mathbb{R}^{2n}} f_i(\overline{a},\overline{b}) \tag{18}$$

under the constraints

$$b(t) \le a(t), \tag{19}$$

$$a(t) \le a,\ b(t) \ge -a,\ t \in [0,T]. \tag{20}$$

Remark 2 *In the case of the Lebesgue square norm we can decompose the object function*

$$\begin{aligned} f_i(\overline{a},\overline{b}) &= \int_{-a}^{a}|q(\overline{a},\overline{b})(u_1)|^2\mathrm{d}u_1 \\ &- 2\left(\int_{-a}^{a} q(\overline{a},\overline{b})(u_1)\Psi_i(u_1)\mathrm{d}u_1\right) + \int_{-a}^{a}\Psi_i(u_1)^2\mathrm{d}u_1. \end{aligned} \tag{21}$$

Denoting

$$I_1(\overline{a},\overline{b}) := \int_{-a}^{a}|q(\overline{a},\overline{b})(u_1)|^2\mathrm{d}u_1, \tag{22}$$

$$I_{2i}(\overline{a},\overline{b}) := -2\left(\int_{-a}^{a} q(\overline{a},\overline{b})(u_1)\Psi_i(u_1)\mathrm{d}u_1\right) \tag{23}$$

the object function f_i is

$$f_i(\overline{a},\overline{b}) = I_1(\overline{a},\overline{b}) + I_{2i}(\overline{a},\overline{b}) + \int_{-a}^{a}\Psi_i(u_1)^2\mathrm{d}u_1.$$

3.2 Optimal solution for the total leaf control

In section 3.1 we considered one individual leaf pair. We shall now consider the control of all leaves applying the scheme of section 3.1. As mentioned above it sufficies to consider only one field. As in section 3.1 we assume that a_i and b_i can be expressed as linear combinations

$$a_i(t) = \sum_{k=1}^{n} a_{ik}\phi_k(t), \tag{24}$$

$$b_i(t) = \sum_{k=1}^{n} b_{ik}\phi_k(t) \tag{25}$$

for $i = 1, ..., N$. We denote $\overline{a}_i = (a_{i1}, ..., a_{in})$, $\overline{b}_i = (b_{i1}, ..., b_{in}) \in \mathbb{R}^n$, $i = 1, ..., N$.

For an individual leaf pair we obtained the object function

$$f_i(\overline{a}_i, \overline{b}_i) = ||q(\overline{a}_i, \overline{b}_i)(\cdot) - \Psi_i||. \tag{26}$$

For the total leaf control problem we choose the object function $F : \mathbb{R}^{2nN} \mapsto \mathbb{R}$ such that

$$F(\overline{a}_1, ..., \overline{a}_N, \overline{b}_1, ..., \overline{b}_N) = \sum_{i=1}^{N} f_i(\overline{a}_i, \overline{b}_i), \tag{27}$$

and the earlier expressed restrictions (section 3.1)

$$b_i(t) \leq a_i(t), \tag{28}$$

$$a_i(t) \leq a,\ b_i(t) \geq -a,\ i = 1, ..., N,\ t \in [0, T]. \tag{29}$$

The real situation in the case of overall leaf configuration implies some additional constraints. The additional constraints might be, for example ([20])

$$a_i(t) \geq -\kappa,\ b_i(t) \leq \kappa,\ i = 1, ..., N,\ t \in [0, T], \tag{30}$$

$$a_i(t) - b_i(t) \geq \overline{\gamma} \text{ or } a_i(t) - b_i(t) = 0,\ i = 1, ..., N,\ t \in [0, T]$$

which under (28) is equivalent to

$$(a_i(t) - b_i(t))(a_i(t) - b_i(t) - \overline{\gamma}) \geq 0,\ i = 1, ..., N,\ t \in [0, T]. \tag{31}$$

Furthermore, the leaf movements may be limited by the constraints

$$b_i(t) \leq a_{i+1}(t),\ b_{i+1}(t) \leq a_i(t),\ i = 1, ..., N-1,\ t \in [0, T], \tag{32}$$

$$a_i(t) - a_j(t) \leq \gamma,\ b_i(t) - b_j(t) \leq \gamma,\ i, j = 1, ..., N,\ t \in [0, T] \tag{33}$$

Above γ, $\overline{\gamma}$ and κ are positive numbers. The condition (30) is needed because the movement of the leaves over the central axis of the field is restricted. The condition (31) means that the opposite leaves are not too near each other or they are closed. Conditions (32-33) are so called interleaf conditions.

Hence the total leaf control problem can be stated as follows:
Find the global minimum

$$\min_{(\overline{a}_1, ..., \overline{a}_N, \overline{b}_1, ..., \overline{b}_N) \in \mathbb{R}^{2nN}} F(\overline{a}_1, ..., \overline{a}_N, \overline{b}_1, ..., \overline{b}_N) \tag{34}$$

under the constraints (28-33).

Besides the above constraints we are able to add other limitations for the trajectories a_i, b_i, for example the unidirectionality of leaves. We can also use weight factors with the above object function.

3.3 A basis system of $\phi_k = \chi_k$

Consider the following possibility to choose the basis system $\{\phi_1, ..., \phi_n\}$. Let $\{t_1, ..., t_n\}$ be a partition of the interval $[0, T]$ and let χ_k be the characteristic function of the subinterval $[t_{k-1}, t_k]$, $k = 1, ..., n$, that is

$$\chi_k(t) = \begin{cases} 1, & t \in [t_{k-1}, t_k] \\ 0, & \text{otherwise} \end{cases}.$$

We choose the computationally simplest case $\phi_k = \chi_k$. This choice of basis is especially useful in the case of multiple static treatment techniques (section 5.1). Here we note that the constraints with respect to this basis can easily be computed. Since $a_i(t) = a_{ik}$, $b_i(t) = b_{ik}$ for $t \in [t_{k-1}, t_k]$ and 0 otherwise the constraints (28-33) are equivalent to the following conditions:

$$b_{ik} \leq a_{ik}, \ i = 1, ..., N, \ k = 1, ..., n \tag{35}$$

$$a_{ik} \leq a, \ b_{ik} \geq -a, \ i = 1, ..., N, \ k = 1, ..., n \tag{36}$$

$$a_{ik} \geq -\kappa \ \text{ and } b_{ik} \leq \kappa, \ i = 1, ..., N, \ k = 1, ..., n \tag{37}$$

$$(a_{ik} - b_{ik})(a_{ik} - b_{ik} - \overline{\gamma}) \geq 0, \ i = 1, ..., N, \ k = 1, ..., n \tag{38}$$

$$b_{ik} \leq a_{(i+1)k}, \ b_{(i+1)k} \leq a_{ik}, \ i = 1, ..., N-1, \ k = 1, ..., n \tag{39}$$

$$a_{ik} - a_{jk} \leq \gamma, \ b_{ik} - b_{jk} \leq \gamma, \ i, j = 1, ..., N, \ k = 1, ..., n. \tag{40}$$

Remark 3 *The total leaf control for several fields $S_l, l = 1, ..., L$ is reduced to the total leaf control for one field since the corresponding intensity distributions Ψ_l are independent in the case where the intensities Ψ_l are precalculated. We optimize each field separately applying the above scheme.*

In section 5.3 we shall give examples for the choice of basis system ψ_j, $j = 1, ..., r$ in such the way that the above quantities in the case of basis system $\phi_k = \chi_k$ can be explicitly calculated.

4 Inverse planning with multileaf parameters

4.1 Inverse problem

Here we express a novel approach to solve the problem of inverse treatment planning with the MLC. The method does not require determination of the intensity distribution as an intermediate step. Specifically, we compute the dose $D = D(x)$ in the patient space with the help of multileaf parameters. Thus we are able to optimize or to find feasible solutions directly by using multileaf parameters.

The patient space is modelled as a three-dimensional interval V typically containing planning target volume (PTV) $\mathbf{T}$, organs at risk (OARs) $\mathbf{C}$ and normal tissue $\mathbf{N}$. We have the mutually disjoint union $V = \mathbf{T} \cup \mathbf{C} \cup \mathbf{N}$. As above the field is modelled as a 2-dimensional interval U. Assume that we have L fields S_l and assume that the corresponding intensity distributions are $\Psi_l, l = 1, ..., L$.

In practise the dose calculations must be done with respect to some fixed coordinate systems. For the origin O of the patient coordinate system (x_1, x_2, x_3) one often chooses the *isocentre point*. The treatment coordinate system (u_1, u_2) is transversally to the line OS_l which connects the isocentre and the *focus*. Figure 2 illustrates these choices. O_l is the intersection of patient surface and the straight line OS_l (field central axis). *Gantry and couch angles* α_l, β_l are the rotation angles with respect to x_3- and x_2- axis, respectively. The *collimator angle* θ_l is the rotation angle with respect to x_1- axis. We fix that $\theta_l = 0$ when u_1- axis is along x_3- axis.

In mathematical modelling of the radiation response by the pencil beam model we apply the integral equation (1). Denote the leaf trajectories of the field S_l by $a_{li}(t)$ and $b_{li}(t)$. Finally, let T_l be the treatment time corresponding to the field S_l.

Using the above definitions the basic problem of the radiation therapy with the help of leaf trajectories can be stated as follows:

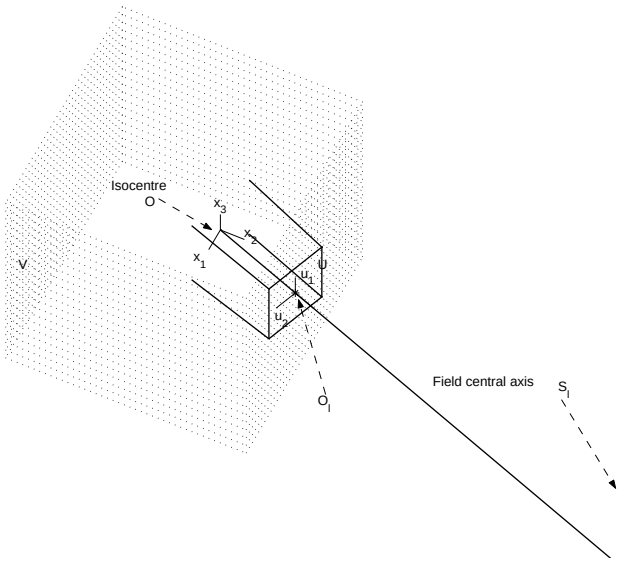

Figure 2: Coordinate systems in dose calculations.

Suppose that D_0 is the prescribed (uniform) dose in $\mathbf{T}$. Furthermore, suppose that the upper bounds of dose in critical organ(s) and normal tissue are D_C and D_N, respectively. Let T_l be positive numbers.

Find the number L of fields S_l, gantry, couch and collimator angles α_l, β_l, θ_l, respectively, of the fields S_l. For any $i = 1, ..., N$, $l = 1, ..., L$ determine under the above described constraints (28-33) the leaf trajectories $a_{li} : [0, T_l] \mapsto \mathbb{R}$, $b_{li} : [0, T_l] \mapsto \mathbb{R}$ of the fields S_l such that the overall dose distribution computed by the integral (1) satisfies

$$\begin{aligned} D(x) &= D_0, \ x \in \mathbf{T}, \\ D(x) &\leq D_C, \ x \in \mathbf{C}, \\ D(x) &\leq D_N, \ x \in \mathbf{N}. \end{aligned} \tag{41}$$

We suppose that parameters L, α_l, β_l are given. In section 6 we consider the determination of collimator angle θ_l. It is expected that the exact solution of the above problem (under the stated or other constraints) does not exist. Hence it reasonable to seek only the approximative but however optimal or feasible solutions of the problem. Here the feasibility of a solution means that instead of the requirement $D(x) = D_0, \ x \in \mathbf{T}$ we demand that

$$d_T \leq D(x) \leq D_T, \ x \in \mathbf{T}$$

where d_T (D_T) is the lower (upper) bound of the dose in PTV.

Besides the requirements (41) one often demands that the so called *dose volume constraints* ([2, 26]) are fulfilled. The dose volume contraints are putted for a certain structure. For example for the critical organs $\mathbf{C}$ these conditions can be shortly described as follows. Let $v(D)$ be the volume fraction of $\mathbf{C}$ that receives a dose greater than D. We demand that

$$v(D) \leq v_0, \text{ for all } D \geq D_0 \tag{42}$$

where v_0 is a given volume fraction and D_0 is a given dose. The function $v = v(D)$ is so called *differential dose volume histogram*. Because the dose volume histogram is a decreasing function with D the condition (42) is equivalent to

$$v(D_0) \leq v_0. \tag{43}$$

In practice the condition (42) must be handled as follows. Take a partition $\{V_m | m = 1, ..., M\}$ of $\mathbf{C}$ and choose $x_m \in \mathbf{C}$. We demand that

$$\frac{count\{m = 1, ..., M | D(x_m) \geq D_0\}}{M} \leq v_0 \tag{44}$$

where *count* denotes the numer of elements of a set. In the case where dose volume contraints are taken into account the conditions like (44) are added to the list (41).

The above given criteria are so called *physical optimization criteria*. In literature there exists also so called *biological optimization criteria*, which are based on the tumor control probality (TCP) and normal tissue complication probality (NTCP) ([2, 26]), for example. Following the formulation of [2] we find that TCP and NTCP can be calculated e.g. by

$$TCP = e^{\int_{\mathbf{T}} \rho(x) \ln(k(D(x)))\, dx} \tag{45}$$

$$NTCP = \frac{1}{\sqrt{2\pi}} \int_{-\infty}^{(< D >_{L^p} - D_{C,50})/\sigma_C} e^{-t^2/2} dt \tag{46}$$

where

$$< D >_{L^p} = \frac{1}{\mu(\mathbf{C})^{1/p}} (\int_{\mathbf{C}} |D(x)|^p dx)^{1/p}.$$

We shall here not consider the optimization based on the biological criteria. So we do not give the detail explanation and optimization schemes for this option. The below done considerations can be rather straightforwardly modified for the optimization strategies based on the biological object functions.

4.2 Optimal solution for the inverse problem

Let U_i be as earlier the strip $[-a, a] \times]u_{2,i-1}, u_{2,i}[$. In section 3 we found that the intensities $\Psi_{li}(u_1)$ in strips U_i corresponding to the field S_l (recall $\Psi_l(u) = \Psi_{li}(u_1),\ u \in U_i$) can be obtained by

$$\Psi_{li}(u_1) = \Psi_0 \int_0^{T_l} H(a_{li}(t) - u_1) H(u_1 - b_{li}(t)) \mathrm{d}t,\ u \in U_i. \tag{47}$$

The strips U_i are mutually disjoint and $U = \cup_{i=1}^N U_i$. Thus we get from (1)

$$D(x) = \sum_{l=1}^{L} \int_U h_l(x, u) \Psi_l(u) \mathrm{d}u = \sum_{l=1}^{L} \sum_{i=1}^{N} \int_{U_i} h_l(x, u) \Psi_{li}(u_1) \mathrm{d}u \tag{48}$$

Substituting (47) to (48) we obtain

$$D(x) = \Psi_0 \sum_{l=1}^{L} \sum_{i=1}^{N} \int_{U_i} \int_0^{T_l} h_l(x, u) H(a_{li}(t) - u_1) H(u_1 - b_{li}(t)) \mathrm{d}t \mathrm{d}u. \tag{49}$$

To get a computable expression for $D(x)$ we use the earlier (sections 7, 3.2) introduced replacement

$$\Psi_{li}(u) = q(\overline{a}_{li}, \overline{b}_{li})(u_1),\ u \in U_i \tag{50}$$

where $\overline{a}_{li} = (a_{li1}, ..., a_{lin_l})$, $\overline{b}_{li} = (b_{li1}, ..., b_{lin_l}) \in \mathbb{R}^{n_l}$ are the *multileaf parameters* for which

$$a_{li}(t) = \sum_{k=1}^{n_l} a_{lik} \phi_{lk}(t),$$

$$b_{li}(t) = \sum_{k=1}^{n_l} b_{lik} \phi_{lk}(t).$$

The basis system $\{\phi_1, ..., \phi_n\}$ may depend on the field S_l so we wrote $\phi_{lk},\ k = 1, ..., n_l$ instead of ϕ_k. From (48) and (50) we obtain

$$D(x) = \sum_{l=1}^{L} \sum_{i=1}^{N} \int_{U_i} h_l(x,u) q(\overline{a}_{li}, \overline{b}_{li})(u_1) \mathrm{d}u. \tag{51}$$

Denote

$$(\mathbf{a}, \mathbf{b}) = (\overline{a}_{11}, ..., \overline{a}_{1N}, ..., \overline{a}_{L1}, ..., \overline{a}_{LN}, \overline{b}_{11}, ..., \overline{b}_{1N}, ..., \overline{b}_{L1}, ..., \overline{b}_{LN}) \in \mathbb{R}^{2N(n_1+...+n_L)}.$$

Furthermore, denote

$$\begin{aligned} D(x, \mathbf{a}, \mathbf{b}) &= \sum_{l=1}^{L} \sum_{i=1}^{N} \int_{U_i} h_l(x,u) q(\overline{a}_{li}, \overline{b}_{li})(u_1) \mathrm{d}u \\ &= \Psi_0 \sum_{l=1}^{L} \sum_{i=1}^{N} \int_{U_i} \int_0^{T_l} h_l(x,u) \tilde{H} \left(\sum_{k=1}^{n_l} a_{lik} \phi_{lk}(t) - u_1 \right) \\ &\quad \cdot \tilde{H} \left(u_1 - \sum_{k=1}^{n_l} b_{lik} \phi_{lk}(t) \right) \mathrm{d}t \mathrm{d}u. \end{aligned} \tag{52}$$

We are able to compute the function $D(x, \mathbf{a}, \mathbf{b})$ when the kernel $h_l(x,u)$ is known. Previously we have developed data fitting methods for determination of the continuous approximations of $h_l(x,u)$ ([9, 18]).

With these concepts we are able to formulate different kind of optimal and feasible problems with the help of multileaf parameters. As an example we consider the following four possibilities. For simplicity (to get the constraints more simple) we assume the step function basis $\phi_k = \chi_k$ given in section 3.3. In addition we have for simplicity specified the used norms in object functions

I. Optimal solution A. Define an object function

$$\begin{aligned} F(\mathbf{a}, \mathbf{b}) &= c_1 ||D_0 - D(\cdot, \mathbf{a}, \mathbf{b})||^2_{L_2(\mathbf{T})} \\ &+ c_2 ||(D_C - D(\cdot, \mathbf{a}, \mathbf{b}))_-||^2_{L_2(\mathbf{C})} + c_3 ||(D_N - D(\cdot, \mathbf{a}, \mathbf{b}))_-||^2_{L_2(\mathbf{N})} \end{aligned} \tag{53}$$

where $c_1,\ c_2,\ c_3$ are positive weights and where the subindex $-$ refers to the negative part of a function.

We state the following extremum problem:

Find the global minimum

$$\min_{(\mathbf{a},\mathbf{b}) \in \mathbb{R}^{2N(n_1+...+n_L)}} F(\mathbf{a}, \mathbf{b}) \tag{54}$$

under the constraints

$$b_{lik} \le a_{lik},\ l = 1, ..., L,\ i = 1, ..., N,\ k = 1, ..., n_l \tag{55}$$

$$a_{lik} \le a,\ b_{lik} \ge -a,\ l = 1, ..., L,\ i = 1, ..., N,\ k = 1, ..., n_l \tag{56}$$

$$a_{lik} \ge -\kappa,\ b_{lik} \le \kappa,\ l = 1, ..., L,\ i = 1, ..., N,\ k = 1, ..., n_l \tag{57}$$

$$(a_{lik} - b_{lik})(a_{lik} - b_{lik} - \overline{\gamma}) \ge 0,\ l = 1, ..., L,\ i = 1, ..., N,\ k = 1, ..., n_l \tag{58}$$

$$b_{lik} \le a_{l(i+1)k},\ b_{l(i+1)k} \le a_{lik},\ l = 1, ..., L,\ i = 1, ..., N-1,\ k = 1, ..., n_l \tag{59}$$

$$a_{lik} - a_{ljk} \le \gamma,\ b_{lik} - b_{ljk} \le \gamma,\ l = 1, ..., L,\ i, j = 1, ..., N,\ k = 1, ..., n_l. \tag{60}$$

II. Feasible solution. In this approach the patient space V is divided into subregions (so called voxels) $V_p,\ p = 1, ..., P$. Suppose that $x_p \in V_p$. Then we have

$$D(x_p) = D(x_p, \mathbf{a}, \mathbf{b}) = \sum_{l=1}^{L} \sum_{i=1}^{N} \int_{U_i} h_l(x_p, u) q(\overline{a}_{li}, \overline{b}_{li})(u_1) \mathrm{d}u. \tag{61}$$

Divide the index set $J = \{1, ..., P\}$ into three disjoint sets $J = J_1 \cup J_2 \cup J_3$ where

$$J_1 = \{p \in J | x_p \in \mathbf{T}\},$$

$$J_2 = \{p \in J | x_p \in \mathbf{C}\},$$

$$J_3 = \{p \in J | x_p \in \mathbf{N}\}.$$

Let $D_N,\ D_C,\ D_T$ be the prescribed upper limit of dose in normal, critical and tumor tissue, respectively and let d_T be the lower limit of dose in tumor tissue.

Then we can state the following feasible problem:
Find $(\mathbf{a}, \mathbf{b}) \in \mathbb{R}^{2N(n_1+...+n_L)}$ *for which the inequalities*

$$d_T \leq D(x_p, \mathbf{a}, \mathbf{b}) \leq D_T,\ p \in J_1, \tag{62}$$

$$D(x_p, \mathbf{a}, \mathbf{b}) \leq D_C,\ p \in J_2, \tag{63}$$

$$D(x_p, \mathbf{a}, \mathbf{b}) \leq D_N,\ p \in J_3, \tag{64}$$

are satisfied under the constraints (55-60).

In addition to the requirements (62-64) one can add the dose volume constraint for the critical organs

$$\frac{count\{p \in J_2 | D(x_p, \mathbf{a}, \mathbf{b}) \leq D_0\}}{count(J_2)} \leq v_0 \tag{65}$$

and similarly for the normal tissue.

III. Optimal solution B. Besides of problem I we can state the corresponding discrete version. Define an object function

$$\begin{aligned} F(\mathbf{a}, \mathbf{b}) &= c_1 \sum_{p \in J_1} |D_0 - D(x_p, \mathbf{a}, \mathbf{b})|^2 \\ &+ c_2 \sum_{p \in J_2} |(D_C - D(x_p, \mathbf{a}, \mathbf{b}))_-|^2 \\ &+ c_3 \sum_{p \in J_3} |(D_N - D(x_p, \mathbf{a}, \mathbf{b}))_-|^2. \end{aligned} \tag{66}$$

where $c_1,\ c_2,\ c_3$ are positive weights.

IV.Optimal solution C. We refine the optimal solution B to take into account smoothness of the dose distribution in PTV by minimizing the gradient (differences). In addition we insert the penalty for the dose volume constraint of the critical organ. Define an object function

$$\begin{aligned} F(\mathbf{a}, \mathbf{b}) &= c_1 \sum_{p \in J_1} |D_0 - D(x_p, \mathbf{a}, \mathbf{b})|^2 \\ &+ c_2 \sum_{p \in J_2} |(D_C - D(x_p, \mathbf{a}, \mathbf{b}))_-|^2 \\ &+ c_3 \sum_{p \in J_3} |(D_N - D(x_p, \mathbf{a}, \mathbf{b}))_-|^2 \\ &+ c_4 |(v_0 - \frac{count\{p \in J_2 | D(x_p, \mathbf{a}, \mathbf{b}) \geq D_0\}}{count(J_2)})_-|^2 \\ &+ c_5 \sum_{p \in J_1} ||\nabla_x D(x_p, \mathbf{a}, \mathbf{b})||^2, \end{aligned} \tag{67}$$

where ∇_x is the gradient of the dose distribution with respect to x-variable. The gradients can be calculated approximately as differences corresponding to each coordinate direction. $c_1,\ c_2,\ c_3,\ c_4$ and c_5 are positive weights.

For optimal solutions B and C we state:
Find the global minimum

$$\min_{(\mathbf{a},\mathbf{b})\in\mathbb{R}^{2N(n_1+\ldots+n_L)}} F(\mathbf{a},\mathbf{b}) \tag{68}$$

under the constraints (55-60).

The feasible problem can be converted to the extremum problem by replacing the term $c_1\sum_{p\in J_1}|D_0 - D(x_p,\mathbf{a},\mathbf{b})|^2$ by

$$c_1\sum_{p\in J_1}|(D_T - D(x_p,\mathbf{a},\mathbf{b}))_-|^2 + c_2\sum_{p\in J_1}|(D(x_p,\mathbf{a},\mathbf{b}) - d_T)_-|^2$$

(cf. also [7]).

5 Multiple static collimation

5.1 Steplike basis ϕ_{lk}

Multiple static collimation means that corresponding to each field S_l the interval $[0,T_l]$ is divided into n_l subintervals $[t_{l0},t_{l1}],\ldots,[t_{l(n_l-1)},t_{ln_l}]$ and during each subinterval the MLC configuration is fixed. So the whole treatment time will be greater than $T_1+\ldots+T_L$ since the change of the MLC configuration corresponding to the subinterval $[t_{l(k-1)},t_{lk}]$, $k=2,\ldots,n_l$ to the MLC configuration corresponding to the next subinterval takes time. Also the change of field configurations will take time.

Let $\{t_{l0},\ldots,t_{ln_l}\}$ be a partition of the interval $[0,T_l]$. Furthermore, let the basis functions ϕ_{lk} be the characteristic functions

$$\chi_{lk}(t) = \begin{cases} 1, & t\in[t_{l(k-1)},t_{lk}] \\ 0, & \text{otherwise} \end{cases}.$$

Then $a_{li}(t)=\sum_{k=1}^{n_l} a_{lik}\chi_{lk}(t)$, $b_{li}(t)=\sum_{k=1}^{n_l} b_{lik}\chi_{lk}(t)$. The leaf configurations corresponding to the subintervals $[t_{l(k-1)},t_{lk}]$, $k=1,\ldots,n_l$ are called *subfields of the fields* S_l, $l=1,\ldots,L$. The practical interpretation of parameters a_{lik}, b_{lik} is that the edges of the i^{th} leaf pair (B_i,A_i) corresponding to the k^{th} subfield of the l^{th} field are at points b_{lik} and a_{lik}. In the following we give a model which is specifically related to the multiple static collimation and which enables to set the lengths of subfields $t_{lk}-t_{l(k-1)}$ as optimization parameters.

Applying the above choice of basis we find that

$$\begin{aligned} q(\overline{a}_{li},\overline{b}_{li})(u_1) &= \Psi_0\int_0^{T_l}\tilde{H}\left(a_{li}(t)-u_1\right)\tilde{H}\left(u_1-b_{li}(t)\right)\mathrm{d}t \\ &= \Psi_0\sum_{k=1}^{n_l}\int_{t_{l(k-1)}}^{t_{lk}}\tilde{H}\left(\sum_{k=1}^{n_l}a_{lik}\chi_{lk}(t)-u_1\right)\tilde{H}\left(u_1-\sum_{k=1}^{n_l}b_{lik}\chi_{lk}(t)\right)\mathrm{d}t \\ &= \Psi_0\sum_{k=1}^{n_l}\tilde{H}(a_{lik}-u_1)\tilde{H}(u_1-b_{lik})(t_{lk}-t_{l(k-1)}). \end{aligned} \tag{69}$$

We observe that the lengths $\delta t_{lk}:=t_{lk}-t_{l(k-1)}$ of the subintervals $[t_{l(k-1)},t_{lk}]$ can also be chosen parameters in the optimization processes. From practical point of view that possibility is very desirable because with this degree of freedom we may decrease the number of subfields and hence the total treatment time. Thus in the case of steplike basis we replace the quantity $q(\overline{a}_{li},\overline{b}_{li})(u_1)$ by

$$q(\overline{a}_{li},\overline{b}_{li},\delta t_l)(u_1) := \Psi_0\sum_{k=1}^{n_l}\tilde{H}(a_{lik}-u_1)\tilde{H}(u_1-b_{lik})(\delta t_{lk}) \tag{70}$$

where $\delta t_l := (\delta t_{l1},\ldots,\delta t_{ln_l})$. The above stated extremum problems are similar with the exceptions that the optimization is done with respect to $(\mathbf{a},\mathbf{b},\delta t)\in\mathbb{R}^{(2N+1)(n_1+\ldots+n_L)}$ and that the additional constraint

$$0\le\delta t_{lk}\le T_l,\ l=1,\ldots,L,\ k=1,\ldots,n_l \tag{71}$$

is required. Here $\delta t := (\delta t_1, ..., \delta t_L) \in \mathbb{R}^{n_1+...+n_L}$. Instead of (71) one may demand that for some $c_0 > 0$

$$c_0 \leq \delta_{lk} \leq T_l \text{ or } \delta_{lk} = 0$$

which is equivalent to

$$0 \leq \delta t_{lk} \leq T_l, \quad \delta_{lk}(\delta_{lk} - c_0) \geq 0, \ l = 1, ..., L, \ k = 1, ..., n_l \tag{72}$$

This restriction will hinder too short subfields.

In section 4 the dose $D(x, \mathbf{a}, \mathbf{b})$ must be replaced by

$$D(x, \mathbf{a}, \mathbf{b}, \delta t) = \sum_{l=1}^{L} \sum_{i=1}^{N} \int_{U_i} h_l(x, u) q(\overline{a}_{li}, \overline{b}_{li}, \delta t_l)(u_1) \mathrm{d}u \tag{73}$$

when we use δt_{lk} as optimization parameters.

Taking into account (69) we find that

$$D(x, \mathbf{a}, \mathbf{b}, \delta t) = \Psi_0 \sum_{l=1}^{L} \sum_{i=1}^{N} \sum_{k=1}^{n_l} [\int_{U_i} h_l(x, u) \tilde{H}(a_{lik} - u_1) \tilde{H}(u_1 - b_{lik}) \mathrm{d}u] \delta t_{lk} \tag{74}$$

Due to the Remark 1 (74) can (approximately) also be written as

$$D(x, \mathbf{a}, \mathbf{b}, \delta t) = \Psi_0 \sum_{l=1}^{L} \sum_{i=1}^{N} \sum_{k=1}^{n_l} [\int_{U_i} h_l(x, u) (\tilde{H}(a_{lik} - u_1) - \tilde{H}(b_{lik} - u_1)) \mathrm{d}u] \delta t_{lk} \tag{75}$$

If we use the pure Heaviside function H instead of (more realistic) modification $\tilde{H}$ the quantity $q(\overline{a}_{li}, \overline{b}_{li})(u_1)$ is replaced by

$$q(\overline{a}_{li}, \overline{b}_{li}, \delta t_l)(u_1) := \Psi_0 \sum_{k=1}^{n_l} H(a_{lik} - u_1) H(u_1 - b_{lik})(\delta t_{lk}). \tag{76}$$

Since

$$H(a_{lik} - u_1) H(u_1 - b_{lik}) = \begin{cases} 1, & b_{lik} \leq u_1 \leq a_{lik} \\ 0, & \text{otherwise} \end{cases}$$

in the case of the pure Heaviside function the dose $D(x, \mathbf{a}, \mathbf{b}, \delta t)$ can easily be computed as follows

$$\begin{aligned} D(x, \mathbf{a}, \mathbf{b}, \delta t) &= \sum_{l=1}^{L} \sum_{i=1}^{N} \int_{U_i} h_l(x, u) q(\overline{a}_{li}, \overline{b}_{li}, \delta t_l)(u_1) \mathrm{d}u \\ &= \Psi_0 \sum_{l=1}^{L} \sum_{i=1}^{N} \sum_{k=1}^{n_l} [\int_{U_i} h_l(x, u) H(a_{lik} - u_1) H(u_1 - b_{lik})](\delta t_{lk}) \mathrm{d}u \\ &= \Psi_0 \sum_{l=1}^{L} \sum_{i=1}^{N} \sum_{k=1}^{n_l} [\int_{u_{2,i-1}}^{u_{2,i}} \int_{-a}^{a} h_l(x, u) H(a_{lik} - u_1) H(u_1 - b_{lik}) \mathrm{d}u](\delta t_{lk}) \\ &= \Psi_0 \sum_{l=1}^{L} \sum_{i=1}^{N} \sum_{k=1}^{n_l} \left(\int_{b_{lik}}^{a_{lik}} \int_{u_{2,i-1}}^{u_{2,i}} h_l(x, u) \mathrm{d}u_2 \mathrm{d}u_1 \right) \delta t_{lk}. \end{aligned} \tag{77}$$

The substitution of (77) for $D(x, \mathbf{a}, \mathbf{b})$ in the above object functions (53), (66) and (67) gives expressions suitable for computations.

5.2 Dose calculation using a convolution kernel

Here we give an example how the dose function can be explicitly calculated. We consider a (semianalytical) convolution kernel and multiple static collimation.

From (75) we recall that (approximately)

$$D(x,\mathbf{a},\mathbf{b},\delta t)=\Psi_0\sum_{l=1}^{L}\sum_{i=1}^{N}\sum_{k=1}^{n_l}[\int_{U_i}h_l(x,u)(\tilde{H}(a_{lik}-u_1)-\tilde{H}(b_{lik}-u_1))du]\delta t_{lk}. \tag{78}$$

Choose a convolution kernel given in [23, 24]

$$h(x,u)=I(x_3)\sum_{j=1}^{3}\frac{c_j}{\pi\sigma_j(x_3)^2}e^{-((x_1-u_1)^2+(x_2-u_2)^2)/\sigma_j(x_3)^2}. \tag{79}$$

This kernel is corresponding to the situation where the origin of the patient coordinate system is in the point O_l marked in the figure 2 and where the x_3-axis is along the line S_lO. By transforming the coordinate system due to this situation and including the rotation of collimator we find that the kernel of the field S_l becomes

$$h_l(x,u)=I((A_lx)_3)\sum_{k=1}^{3}\frac{c_k}{\pi\sigma_k((A_lx)_3)^2}e^{-(((A_lx)_1-u_1)^2+((A_lx)_2-u_2)^2)/\sigma_k((A_lx)_3)^2}$$

where

$$A_lx=R_{x_1}(\theta_l)^{-1}R_{x_2}(\beta_l+\frac{\pi}{2})^{-1}R_{x_3}(\alpha_l)^{-1}(x-O_l)^T$$

where T refers to the transpose of a matrix and where $R_{x_j},\ j=1,2,3$ are the standard rotation matrices ([26]).

The kernel does not take into account the beam divergence and the tissue inhomogeneities. In addition, the kernel neglects the real patient geometry. It can be applied only for planar patient surfaces and the straight line OS_l must be orthogonal to the patient surface. However these shortcommings can be corrected by considering individual pencil beams. These corrections are not essential here. The parameters $I(x_3),\ c_j,\ \sigma_j(x_3)$ are tabulated in literature ([23]). $I(x_3)$ can alternatively be calcutated from

$$I(x_3)=[d_1+d_2(\mu x_3)^q]e^{-\mu x_3}$$

where parameters $d_1,\ d_2,\ \mu,\ q$ are tabulated ([23]).

Furthermore choose

$$\tilde{H}(x)=\mathrm{erf}_\tau(x). \tag{80}$$

Since for $a<b$

$$\int_a^b e^{-(x-v)^2/\tau^2}\mathrm{d}v=\sqrt{\pi}\tau(\mathrm{erf}_\tau(b-x)-\mathrm{erf}_\tau(a-x))$$

and for all $b_1\le a_1\le a_2\le b_2$ and τ small enough (see Lemma 1 in APPENDIX)

$$\int_{b_1}^{b_2}e^{-(x-v)^2/\sigma^2}(\mathrm{erf}_\tau(a_2-v)-\mathrm{erf}_\tau(a_1-v))\mathrm{d}v\approx\sqrt{\pi}\sigma(\mathrm{erf}_\rho(a_2-x)-\mathrm{erf}_\rho(a_1-x)) \tag{81}$$

where $\rho=\sqrt{\sigma^2+\tau^2}$ we find that (approximately)

$$\begin{aligned}D(x,\mathbf{a},\mathbf{b},\delta t) \quad = \quad & \Psi_0\sum_{l=1}^{L}\sum_{i=1}^{N}\sum_{k=1}^{n_l}\sum_{j=1}^{3}c_jI((A_lx)_3)\\ & [\mathrm{erf}_{\rho_j((A_lx)_3)}(a_{lik}-(A_lx)_1)-\mathrm{erf}_{\rho_j((A_lx)_3)}(b_{lik}-(A_lx)_1))]\\ & \cdot[\mathrm{erf}_{\sigma_j((A_lx)_3)}(u_{2,i}-(A_lx)_2)-\mathrm{erf}_{\sigma_j((A_lx)_3)}(u_{2,i-1}-(A_lx)_2))]\delta t_{lk}\end{aligned} \tag{82}$$

where $\rho_j(x_3)=\sqrt{\sigma_j(x_3)^2+\tau^2}$.

5.3 Polynomial and Fourier basis ψ_j

Here we give some examples how to choose the basis $\{\psi_j |\ j = 1, ..., r\}$ for the replacement (7). We deal with two possibilities, polynomial basis and Fourier basis. The advantage of these choices is that e.g. in multiple static collimation the expression $q(\overline{a}_{li}, \overline{b}_{li}, \delta t_l)$ (and hence Ψ_{li} and some of the above object functions) can be explicitly calculated. It suffices to consider one field and so we omit the subscript l. We shall give only shortly the results because the detail computations are not essential here.

A. Polynomial basis. In this case we choose

$$\tilde{H}(x) = \sum_{j=0}^{r} d_j x^j. \tag{83}$$

Let $\alpha = (\alpha_1, ..., \alpha_n) \in \mathbb{N}_0^n$ be a multi-index and let $|\alpha| = \alpha_1 + ... + \alpha_n$ and $\alpha! = \alpha_1! \cdots \alpha_n!$ for $\alpha \in \mathbb{N}_0^n$. In addition we denote (as above) $\overline{a}_i = (a_{i1} \cdots a_{in})$, $\overline{b}_i = (b_{i1} \cdots b_{in})$ and

$$\overline{\phi}(t) = (\phi_1(t) \cdots \phi_n(t)),\ x^\alpha = x_1^{\alpha_1} \cdots x_n^{\alpha_n}$$

for $\alpha \in \mathbb{N}_0^n$ and $x \in \mathbb{R}^n$.

We have obtained that

$$q(\overline{a}_i, \overline{b}_i)(u_1) = \int_0^T Q_i(u_1, t)\mathrm{d}t = \Psi_0 \sum_{j_1=0}^{r} \sum_{j_2=0}^{r} \sum_{\nu=0}^{j_1} \sum_{\mu=0}^{j_2} p_{j_1,j_2,\nu,\mu}(\overline{a}_i, \overline{b}_i) u_1^{j_1-\nu+\mu} \tag{84}$$

where

$$\begin{aligned} p_{j_1,j_2,\nu,\mu}(\overline{a}_i, \overline{b}_i) &= \sum_{|\alpha|=\nu} \sum_{|\beta|=j_2-\mu} d_{j_1} d_{j_2} \binom{j_1}{\nu} \binom{j_2}{\mu} \frac{\nu!}{\alpha!} \frac{(j_2-\mu)!}{\beta!} \\ &\times \quad (-1)^{j_1+j_2-\nu-\mu} \overline{a}_i^\alpha \overline{b}_i^\beta \Big(\int_0^T \overline{\phi}^\alpha(t) \overline{\phi}^\beta(t)\mathrm{d}t \Big). \end{aligned} \tag{85}$$

The expressions $p_{j_1,j_2,\nu,\mu}(\overline{a}_i, \overline{b}_i)$ are multipolynomials with respect to $(\overline{a}_i,\ \overline{b}_i)$ in $\mathbb{R}^{2n}$.

For the above given steplike basis $\phi_k = \chi_k$ we have

$$p_{j_1,j_2,\nu,\mu}(\overline{a}_i, \overline{b}_i) = d_{j_1} d_{j_2} \binom{j_1}{\nu} \binom{j_2}{\mu} (-1)^{j_1+j_2-\nu-\mu} \sum_{k=1}^{n} a_{ik}^\nu b_{ik}^{j_2-\mu} (\delta t_k). \tag{86}$$

Hence the quantity $q(\overline{a}_i, \overline{b}_i)$ or $q(\overline{a}_i, \overline{b}_i, \delta t)$ can be immediately calculated from (85-86). We recall that in the case of steplike basis also the constraints can be computed.

B. Fourier basis. We assume that $[-a, a] = [-\pi, \pi]$. The more general situation can be straightforwardly reduced to this case by an elementary coordinate transformation. Hence we choose

$$\tilde{H}(x) = \sum_{j=-M}^{M} d_j \mathrm{exp}(\mathrm{i}jx) \tag{87}$$

where $M \in \mathbb{N}$ and i is the imaginary unit. We have obtained that

$$\begin{aligned} q(\overline{a}_i, \overline{b}_i)(u_1) &= \int_0^T Q(u_1, t)\mathrm{d}t = \Psi_0 \sum_{j_1=-M}^{M} \sum_{j_2=-M}^{M} d_{j_1} d_{j_2} \mathrm{exp}[\mathrm{i}(j_2 - j_1)u_1] \\ &\times \quad \int_0^T \prod_{k=1}^{n} \mathrm{exp}(\mathrm{i}(j_1 a_{ik} - j_2 b_{ik})\phi_k(t))\mathrm{d}t. \end{aligned} \tag{88}$$

In the case of steplike basis $\phi_k = \chi_k$ we have

$$\begin{aligned} q(\overline{a}_i, \overline{b}_i, \delta t)(u_1) &= \Psi_0 \sum_{j_1=-M}^{M} \sum_{j_2=-M}^{M} \sum_{k=1}^{n} d_{j_1} d_{j_2} \exp[\mathrm{i}(j_2 - j_1)u_1] \\ &\times \exp[\mathrm{i}(j_1 a_{ik} - j_2 b_{ik})](\delta t_k) \end{aligned} \tag{89}$$

and then $q(\overline{a}_i, \overline{b}_i)$ or $q(\overline{a}_i, \overline{b}_i, \delta t)$ can be computed from (88) or (89). The constraints are considered as above for the steplike basis ϕ_k.

6 Optimizing algorithms and simulations

In real situation the number N of leaf pairs is typically $20 - 25$. Assuming that the number of fields is $L = 3-10$ and that the number n of subfields, is between $5-10$ we find that $2N(n_1+...+n_L) = 600-5000$. Hence the above problem is a large scale optimizing problem. The constraints are mainly linear inequality constraints. The object function F is defined in a subset of $\mathbb{R}^{2N(n_1+...+n_L)}$ and it is nonlinear. So the optimizing algorithm must be chosen so that it is specified for nonlinear optimizing problems with constraints. In addition, the large dimensionality of the problem must be taken into account. The algorithm must be carefully initialized (all possible apriori information must be taken into account) or it must have a capability to search global extremums. Here we consider the problem by applying the first alternative.

6.1 Choice of collimator angle. Initialization of optimization for multiple static collimation

At first we calculate relevant initial values for the locations of multileaf parameters $(\mathbf{a}, \mathbf{b})$ and for the lenghts of subfields δt to ensure that the solution is close to the global minimum of the object function $F(\mathbf{a}, \mathbf{b}, \delta t)$. In addition we select the collimator angle according to some criteria optimally. We suggest the following procedure which is divided into four subsequent steps.

1. Choose the collimator angle "optimally" and take into account the leaf constraints. The collimator "sees" only the 3-dimensional orthogonal (field's eye view) projection of the patient domain onto the transversal collimator plane. For each field S_l there exists an unique minimal rectangle $U_l := [a_1^l, a_2^l] \times [b_1^l, b_2^l] \subset U$ inside which the projection of the patient domain is situated (figure 3). The minimal rectangle and the locations of leaf heads are dependent on the collimator angle θ.

   Set the collimator leaves most conformally for PTV. Figure 4 illustrates this step. Denote the locations of leaf heads corresponding to the angle θ by

$$\begin{aligned} (\mathbf{a}(\theta), \mathbf{b}(\theta)) &= (a_{11}(\theta), ..., a_{1N}(\theta), ..., a_{L1}(\theta), ..., a_{LN}(\theta), \\ &\quad b_{11}(\theta), ..., b_{1N}(\theta), ..., b_{L1}(\theta), ..., b_{LN}(\theta)). \end{aligned} \tag{90}$$

   For each field the optimal selection of the collimator angle could mean that e.g. the following facts are taken into account

   (a) Rotate the collimator such that the u_1-side of the minimal rectangle is minimal. This choice diminish the movements of leaves. In addition this choice may improve the benefits of back up diaphragms to decrease the leakage between the leaves. The proposed choice is not necessarily the best one (cf. [22]). For this option we set the penalty term

$$f_1(\theta) = c_1(\min_{1 \le i \le N} b_{li}(\theta) - \max_{1 \le i \le N} a_{li}(\theta)). \tag{91}$$

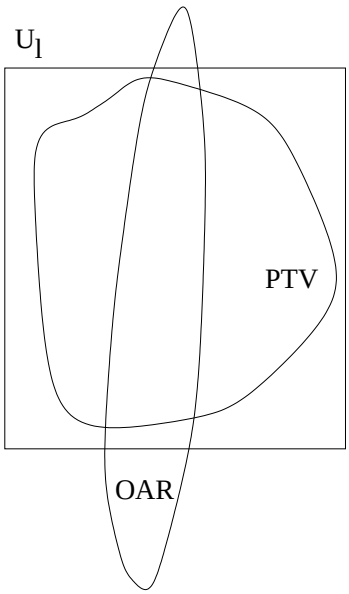

Figure 3: The orthogonal projection onto the collimator plane of the 3-dimensional patient data corresponding to the field S_l. The minimum rectangle U_l is shown.

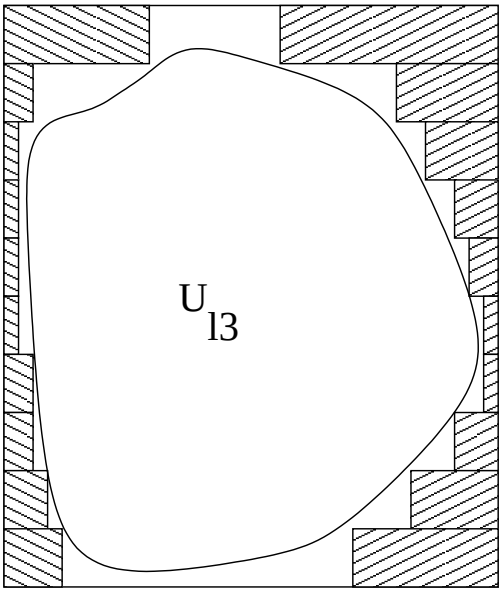

Figure 4: The conformal setting of leaves corresponding to the field S_l. U_{l3} is the region between the multileaf steplike outline corresponding to subfield S_{l3}.

(b) Minimize the area between the outline of PTV and the multileaf steplike outline. By minimizing this area we improve the conformality. For this option we set the penalty term

$$f_2(\theta) = c_2(\sum_{1\le i\le N}(a_{li}(\theta) - b_{li}(\theta))d - A).$$

Here $\sum_{1\le i\le N}(a_{li}(\theta)-b_{li}(\theta))d$ is the area inside the multileaf steplike outline and A is the area inside the PTV outline. Since A is independent of θ we can replace $f_2(\theta)$ by

$$f_2(\theta) = c_2(\sum_{1\le i\le N}(a_{li}(\theta) - b_{li}(\theta))). \tag{92}$$

(c) Take into account the leaf constraints. We penalize if the leaf constraints are violated and then we put the following penalty term (note that the physically impossible constraints (55, 56) are omitted)

$$\begin{aligned} f_3(\theta) &= c_4\sum_{i=1}^{N}(\max(0,-(a_{li}(\theta)+\kappa))^p \\ &+ c_5\sum_{i=1}^{N}(\max(0,b_{li}(\theta)-\kappa))^p \\ &+ c_6\sum_{i=1}^{N}(\max(0,-(a_{li}(\theta)-b_{li}(\theta))(a_{li}(\theta)-b_{li}(\theta)-\overline{\gamma})))^p \\ &+ c_7\sum_{i,j=1}^{N}(\max(0,a_{li}(\theta)-a_{lj}(\theta)-\gamma))^p \\ &+ c_8\sum_{i,j=1}^{N}(\max(0,b_{li}(\theta)-b_{lj}(\theta)-\gamma)))^p \\ &+ c_9\sum_{i=1}^{N-1}(\max(0,b_{li}(\theta)-a_{l(i+1)}(\theta)))^p \\ &+ c_{10}\sum_{i=1}^{N-1}(\max(0,b_{l(i+1)}(\theta)-a_{li}(\theta)))^p. \end{aligned} \tag{93}$$

Above p is a positive integer.

(d) Save the critical organs and the healthy tissue inside the PTV. Simultaneously minimize the area of PTV covered by MLC. We omit this option here.

(e) Other criteria, e.g. take into account the dose gradients (cf. [22])

The choice of collimator angle for an individual field S_l is the solution of the extremum problem

$$\min_{\theta\in[0,2\pi]}(f_1(\theta)+f_2(\theta)+f_3(\theta)). \tag{94}$$

After this step the leaf settings are

$$\begin{aligned} (\tilde{\mathbf{a}}_0,\tilde{\mathbf{b}}_0) &:= (\tilde{a}^0_{11},...,\tilde{a}^0_{1N},...,\tilde{a}^0_{L1},...,\tilde{a}^0_{LN},\tilde{b}^0_{11},...,\tilde{b}^0_{1N},...,\tilde{b}^0_{L1},...,\tilde{b}^0_{LN}) \\ &:= (\mathbf{a}(\theta_0),\mathbf{b}(\theta_0)) \end{aligned} \tag{95}$$

where θ_0 is the minimum point of (94).

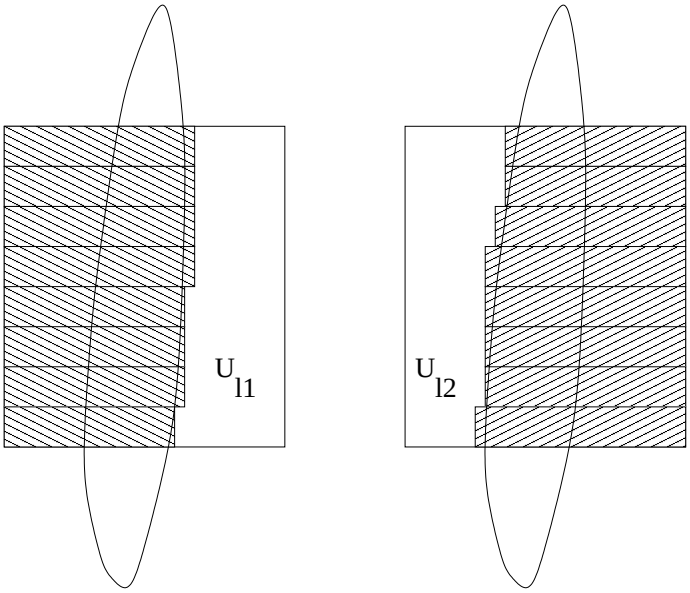

Figure 5: The setting of leaves during the subfields $S_{lk},\ k = 1, 2$. $U_{lk},\ k = 1, 2$ are regions between the multileaf steplike outline.

2. To save the critical organ **C** inside the projection of PTV we suggest the following method. Suppose that each field S_l contains (at most) n_l subfields $S_{lk},\ k = 1, ..., n_l$. Let $0 \leq m_l \leq n_l$. During the subfields $S_{lk},\ k = 1, ..., m_l$ put the leaves subsequently as illustrated in figure 5. During the subfields $S_{lk},\ k = m_l + 1, ..., n_l$ put the leaves as in step 1. Take into account the leaf constraints. If some of the leaf constraints would be violated use as well as possible settings such that the constraints are not violated.

   In the following we consider a special case which can be applied for the critical organs with serial structure. We assume that $n_l = 3,\ l = 1, ..., L$ and $m_l = 2,\ l = 1, ..., L$. The leaf configurations of the first two subfields $S_{l1},\ S_{l2}$ are illustrated in figure 5 and during the last subfield S_{l3} the leaf configuration is as in figure 4.

   Denote the lenghts of the subfields $S_{lk},\ k = 1, 2, 3$ by δ_{lk}. We seek a feasible solution for the lenghts δ_{lk} as follows. Let U_{lk} be the *open fields* corresponding to the subfields S_{lk} (see figures 4 and 5). Furthermore, let the corresponding leaf locations be

$$(a^0_{11k}, ..., a^0_{1Nk}, ..., a^0_{L1k}, ..., a^0_{LNk}, b^0_{11k}, ..., b^0_{1Nk}, ..., b^0_{L1k}, ..., b^0_{LNk})$$

   Denote (as above)

$$\overline{a}^0_{li} = (a^0_{li1}, a^0_{li2}, a^0_{li3}),\ \overline{b}^0_{li} = (b^0_{li1}, b^0_{li2}, b^0_{li3})$$

   and

$$(\mathbf{a}_0, \mathbf{b}_0) = (\overline{a}^0_{11}, ..., \overline{a}^0_{1N}, ..., \overline{a}^0_{L1}, ..., \overline{a}^0_{LN}, \overline{b}^0_{11}, ..., \overline{b}^0_{1N}, ..., \overline{b}^0_{L1}, ..., \overline{b}^0_{LN}).$$

   We omit the above mentioned corrections in dose calculation. We calculate the dose per unit time and corresponding to this open subfield by

$$D_{lk}(x) = \Psi_0 \int_{U_{lk}} h_l(x, u) \mathrm{d}u \tag{96}$$

   (see (77)). Here we use the convolution kernel $h_l(x, u)$ of section 5

As in section 5.2 we obtain that the dose per unit time of these subfields is

$$\begin{aligned} D_{lk}(x) &= \Psi_0 \sum_{i=1}^{N}\sum_{j=1}^{3} c_j I((A_l x)_3) \\ &\cdot[\mathrm{erf}_{\sigma_j((A_l x)_3)}(a^0_{lik} - (A_l x)_1) - \mathrm{erf}_{\sigma_j((A_l x)_3)}(b^0_{lik} - (A_l x)_1)] \\ &\cdot[\mathrm{erf}_{\sigma_j((A_l x)_3)}(u_{2,i} - (A_l x)_2) - \mathrm{erf}_{\sigma_j((A_l x)_3)}(u_{2,i-1} - (A_l x)_2)]. \end{aligned} \tag{97}$$

Hence the total dose is

$$D(x) = \sum_{l=1}^{L}\sum_{k=1}^{3} D_{lk}(x)\delta t_{lk}. \tag{98}$$

We use the notations of section 4.2. Assume that

$$J_1 = \{1, ..., m_1\},\ J_2 = \{m_1 + 1, ..., m_2\},\ J_3 = \{m_2 + 1, ..., P\}.$$

The feasible problem requires

$$d_T \le D(x_p) \le D_T,\ p = 1, ..., m_1$$

$$D(x_p) \le D_C,\ p = m_1 + 1, ..., m_2$$

$$D(x_p) \le D_N,\ p = m_2 + 1, ..., P$$

and naturally

$$0 \le \delta t_{lk} \le T_l. \tag{99}$$

The problem can be written in the matrix form

$$H(\mathbf{x})\delta t \le \mathbf{b} \tag{100}$$

where $H(\mathbf{x})$ is $((P + m_1 + 6L)) \times (3L))$- matrix

$$H(\mathbf{x}) = \left(\tilde{H}(\mathbf{x}) \ -\mathbf{I}\ \mathbf{I}\right)^{\mathrm{T}},$$

where T refers to a transpose of a matrix. Here $\mathbf{I}$ is the $(3L \times 3L)$ unit matrix and

$$\tilde{H}(\mathbf{x}) = \left(H_1(\mathbf{x}) \ \cdots \ H_L(\mathbf{x})\right)$$

where

$$H_l(\mathbf{x}) = \begin{pmatrix} D_{l1}(x_1) & D_{l2}(x_1) & D_{l3}(x_1) \\ \vdots & \vdots & \vdots \\ D_{l1}(x_{m_1}) & D_{l2}(x_{m_1}) & D_{l3}(x_{m_1}) \\ -D_{l1}(x_1) & -D_{l2}(x_1) & -D_{l3}(x_1) \\ \vdots & \vdots & \vdots \\ -D_{l1}(x_{m_1}) & -D_{l2}(x_{m_1}) & -D_{l3}(x_{m_1}) \\ D_{l1}(x_{m_1+1}) & D_{l2}(x_{m_1+1}) & D_{l3}(x_{m_1+1}) \\ \vdots & \vdots & \vdots \\ D_{l1}(x_{m_2}) & D_{l2}(x_{m_2}) & D_{l3}(x_{m_2}) \\ D_{l1}(x_{m_2+1}) & D_{l2}(x_{m_2+1}) & D_{l3}(x_{m_2+1}) \\ \vdots & \vdots & \vdots \\ D_{l1}(x_P) & D_{l2}(x_P) & D_{l3}(x_P) \end{pmatrix} \tag{101}$$

$$\delta t = \left(\ \delta t_{11} \quad \delta t_{12} \quad \delta t_{13} \quad \cdots \quad \delta t_{L1} \quad \delta t_{L2} \quad \delta t_{L3},\ \right)^{\mathrm{T}}$$

$$\mathbf{b} = (D_T \ \cdots \ D_T \ -d_T \ \cdots \ -d_T \ D_C \ \cdots \ D_C \ D_N \ \cdots \ D_N \ \mathbf{0} \ \mathbf{q})^{\mathrm{T}}$$

Here $\mathbf{0} = (0, ..., 0) \in \mathbb{R}^{3L}$ and where $\mathbf{q} = (T_1, T_1, T_1, ..., T_L, T_L, T_L) \in \mathbb{R}^{3L}$. Here T_l may be e.g. $\frac{T}{L}$. Since for the open field the connection $D_0 = cT$ is known we can calculate T.

The feasible problem (100) is solved by the Cimmino algorithm ([3, 9]). Denote the solution by

$$\delta t_0 = (\delta t_{11}^0, \delta t_{12}^0, \delta t_{13}^0, ..., \delta t_{L1}^0, \delta t_{L2}^0, \delta t_{L3}^0) \in \mathbb{R}^{3L}.$$

3. If necessary, shield the healthy tissue $\mathbf{N}$ inside the projection of PTV as in step 2 the OAR was shielded.

4. The initial point is
$$(\mathbf{a}_0, \mathbf{b}_0, \delta t_0). \tag{102}$$
In the actual optimization we put (to save the conformality) the additional constraint
$$a_{lik} \leq \tilde{a}_{li}^0, \ b_{lik} \geq \tilde{b}_{li}^0 \tag{103}$$
for $l = 1, ..., L, \ i = 1, ..., N, \ k = 1, 2, 3$. The constraints $a_{lik} \leq a, \ b_{lik} \geq -a$ can be removed.

6.2 Search of feasible solution for the linearized problem

In this contribution we apply the feasible solution approach (Problem II of section 4.2). The actual optimization is also solved by the Cimmino algorithm. At first we linearize the dose function $D(x_p, \mathbf{a}, \mathbf{b}, \delta t)$ at the initial point $(\mathbf{a}_0, \mathbf{b}_0, \delta t_0)$ that is

$$\begin{aligned} D(x_p, \mathbf{a}, \mathbf{b}, \delta t) &\approx D(x_p, \mathbf{a}_0, \mathbf{b}_0, \delta t_0) + J_D(x_p, \mathbf{a}_0, \mathbf{b}_0, \delta t_0) \begin{pmatrix} (\mathbf{a} - \mathbf{a}_0)^{\mathrm{T}} \\ (\mathbf{b} - \mathbf{b}_0)^{\mathrm{T}} \\ (\delta t - \delta t_0)^{\mathrm{T}} \end{pmatrix} \\ &= : f(x_p, \mathbf{a}_0, \mathbf{b}_0, \delta t_0) + J_D(x_p, \mathbf{a}_0, \mathbf{b}_0, \delta t_0) \begin{pmatrix} \mathbf{a}^{\mathrm{T}} \\ \mathbf{b}^{\mathrm{T}} \\ \delta t^{\mathrm{T}} \end{pmatrix} \end{aligned} \tag{104}$$

where $J_D(x_p, \mathbf{a}_0, \mathbf{b}_0, \delta t_0)$ is the Jacobian matrix of $D(x_p, \mathbf{a}, \mathbf{b}, \delta t)$ with respect to the variable $(\mathbf{a}, \mathbf{b}, \delta t)$. Since the dose function D is real valued we in fact have

$$J_D(x_p, \mathbf{a}_0, \mathbf{b}_0, \delta t_0) \begin{pmatrix} \mathbf{a}^{\mathrm{T}} \\ \mathbf{b}^{\mathrm{T}} \\ \delta t^{\mathrm{T}} \end{pmatrix} = \langle \nabla D(x_p, \mathbf{a}_0, \mathbf{b}_0, \delta t_0), (\mathbf{a}, \mathbf{b}, \delta t) \rangle.$$

Denote $f_p := f(x_p, \mathbf{a}_0, \mathbf{b}_0, \delta t_0)$

The corresponding feasible problem states:

Find $(\mathbf{a}, \mathbf{b}, \delta t) \in \mathbb{R}^{6NL+3L}$ *for which the inequalities*

$$d_T - f_p \leq J_D(x_p, \mathbf{a}_0, \mathbf{b}_0, \delta t_0) \begin{pmatrix} \mathbf{a}^{\mathrm{T}} \\ \mathbf{b}^{\mathrm{T}} \\ \delta t^{\mathrm{T}} \end{pmatrix} \leq D_T - f_p, \ p \in J_1, \tag{105}$$

$$J_D(x_p, \mathbf{a}_0, \mathbf{b}_0, \delta t_0) \begin{pmatrix} \mathbf{a}^{\mathrm{T}} \\ \mathbf{b}^{\mathrm{T}} \\ \delta t^{\mathrm{T}} \end{pmatrix} \leq D_C - f_p, \ p \in J_2, \tag{106}$$

$$J_D(x_p, \mathbf{a}_0, \mathbf{b}_0, \delta t_0) \begin{pmatrix} \mathbf{a}^{\mathrm{T}} \\ \mathbf{b}^{\mathrm{T}} \\ \delta t^{\mathrm{T}} \end{pmatrix} \leq D_N - f_p, \ p \in J_3, \tag{107}$$

are satisfied under the constraints (55-60) , (71) (or (72)) and (103).

We remove the nonlinear constraints (58) and (72). If we took into account these constraints we ought to linearize them at the initial point. The feasible solution (105-107) with the mentioned constraints can be solved with the Cimmino algorithm as above. We omit the detailed formulations since the principles are presented in the previous considerations. However, we mention that the additional constraints

$$a^0_{lik} - \kappa_1 \leq a_{lik} \leq a^0_{lik} + \kappa_1$$

$$b^0_{lik} - \kappa_1 \leq b_{lik} \leq b^0_{lik} + \kappa_1$$

$$\delta t^0_{lk} - \kappa_2 \leq \delta t_{lk} \leq \delta t^0_{lk} + \kappa_2$$

are required, where κ_1 and κ_2 are so small that the feasible solution of the original nonlinear problem (62-64) is expected to achieved. Since the original problem is nonlinear it is recommended that the linearization point is changed after some iterations. The new linearization point is the solution obtained in the previous iteration.

The dose volume constraints can also be taken into account in this optimization method. We omit details here.

6.3 Simulations

In simulations we studied the introduced methods. The combined triple Gaussian pencil beam kernel (section 5.2) and MLC scatter model (section 3.1) were used in the solution of the inverse problem of radiotherapy treatment planning. In the inverse problem both leaf positions ($\mathbf{a}$, $\mathbf{b}$) and irradiation times δt were solved to get a feasible dose distribution.

The course of the solution of the inverse problem is as follows.

1. Place treatment fields and give dose limits for PTV and OAR.
2. Determine initial leaf positions using patient geometry (section 6.1). Also the number of subfields is decided.
3. Compute the dose deposition kernel (101) for the determined subfields using triple Gaussian pencil beam and MLC scattering models.
4. Find a feasible solution for the irradiation times δt of the subfields (cf. [9]).
5. Check the solution. If it is good enough, stop.
6. If the solution is not satisfactory, solve the system of nonlinear inequalities for leaf positions and irradiation times using the linearization in Cimmino algorithm as described in section 6.2. After each iteration check whether the solution is good enough. If not, go to next iteration round.

In the last step of the solution process at each iteration the modifications of the leaf positions are solved first and *after* this the irradiation times are determined according to the changed leaf patterns. This is because of the linear character of δt and nonlinear character of $\mathbf{a}$, $\mathbf{b}$.

One PTV – OAR situation was studied. A C-shaped PTV was partly surrounding a smaller OAR (figure 6). Concave dose distribution was demanded. The PTV and the OAR were in a box-shaped water phantom.

Two and five fields were used. One of the two fields had gantry angle 0 degrees and the other 152 degrees. Five fields were equiangled, coplanar and isocentric. Field sizes were governed by the PTV projections in the field determination planes which were placed at the isocenter orthogonally to the central axes of the fields. The photon energy for the fields was 6 MV as the parameters needed by the triple Gaussian dose calculation model are tabulated in [24]. Collimator angles of the fields were not optimized. The number of leaf pairs was $N = 3$ in both simulations.

Dose constraints were same in both cases. Relative dose in the PTVs was limited between 95 – 110 % and in the OARs under 60 %. The PTV lower and the OAR higher limits were weighted twice the amount the higher dose constraint of the PTV.

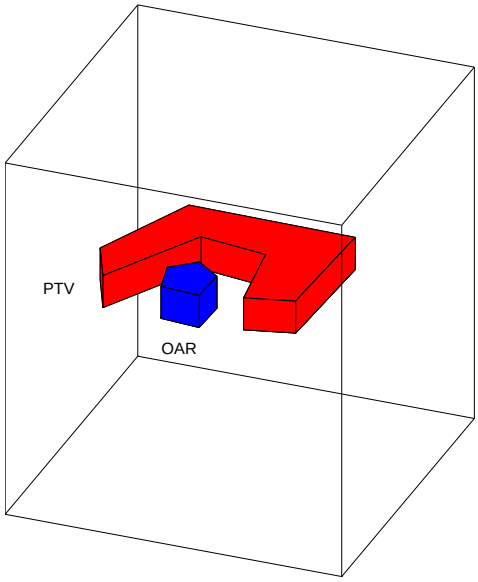

Figure 6: The phantom that was used in the simulations.

The MLC has technical constraints. In these simulations the virtual MLC had the following limitations: Leaves could not move outside the field (56), leaves were not allowed to collide (55) and the interleaf situation (59) was prohibited.

Figure 7 shows the results of the inverse solution for the first case and figure 8 for the second. Better conformation, of course, is obtained using five fields. Notice that the dose to the rest of the phantom (normal tissue) was not constrained. Both cases were run 10 iterations; after this the solutions did not improve significantly. In the two-field simulation the minimum and maximum dose in the PTV were 80.1 % and 120.5 % respectively. The highest dose in the OAR was 75.4 %. In the five-field case the minimum and maximum in the PTV were 90.4 % and 113.5 % respectively. The highest dose in the OAR was 66.0 %.

7 Conclusions

In the present study we have suggested one model to control the leaves of MLC. In addition we have expressed the idea how the inverse treatment planning in radiation therapy can be done directly by controlling the leaves of MLC. The study is preliminary and there are many details demanding more study and improvements. Especially the applied optimizing (computational) algorithms must be further developed. The application of so-called global optimization algorithms and the initialization as accurately as possible are helpfull in the optimization.

In this contribution we applied the initialization based on the geometrical intuition. The other alternative for the initialization is to determine an approximation for the intensity and set the leaves according to this information as described in [20]. This initialization method will be studied in the subsequent research.

The simulations were done in reduced dimensions (that is reduced values of N) but the generalizations to real dimensions are straightforward. In real dimensions the computational complexity will increase and our aim is to develope more effective computational tools for this case. Furthermore the head scatter and leakage effects must be included to the model more accurately.

It is obvious that applying MLC using multiple static method we can not produce arbitrarily shaped intensity modulations. We will in the future develope and test the control of the MLC in the inverse problem. Our method ensures that the MLC constraints are properly taken into account when the

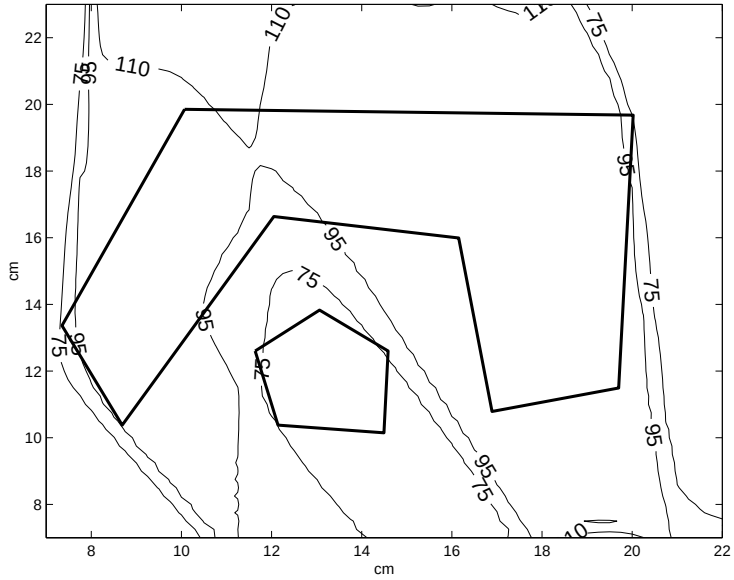

Figure 7: Dose distribution in a transversal plane in the two-field case. Isodoses represent the dose.

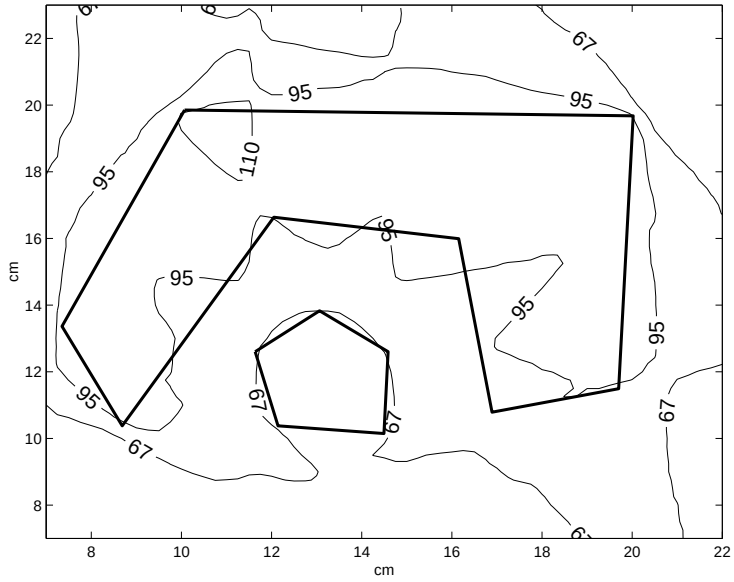

Figure 8: Dose distribution in a transversal plane in the five-field case. Isodoses represent the dose.

inverse problem is solved. Moreover the head scattering, leakage and groove and tongue effects can be more accurately modelled when we optimize directly the MLC parameters.

In this (and previous) papers we have introduced some of the mathematical tools needed to create intensity modulated treatment plans. There are however two major parts of our inverse method that need to be thoroughly tested before the method will be applied into practice. The first is the approximation for the dose deposition kernel $h_l(x,u)$. The second is the head scattering and leakage model that will replace the Heaviside function.

We have implemented the multiple static treatment technique. Modifying our model there are also other kind of possibilities to deliver the dose, e.g. the dynamic collimation. In the dynamic collimation the limited velocity and acceleration of leaves bring up restrictions. We skecth how our algorithms can be modified to include dynamic delivery techniques.

In the cases where the velocity of the leaf trajectories contains limitations we assume that the velocities $v_A(t),\ v_B(t)$ of opposite leaves (say A and B) can be expressed as linear combinations

$$v_A(t) = \sum_{k=1}^{n} a_k \phi_k(t),\ v_B(t) = \sum_{k=1}^{n} b_k \phi_k(t)$$

with respect to a suitable basis $\{\phi_1, ..., \phi_n\}$. Then the leaf trajectories $a(t)$ and $b(t)$ can be obtained as integrals

$$a(t) = a_0 + \int_0^t v_A(\tau)\mathrm{d}\tau = a_0 + \sum_{k=1}^{n} a_k \int_0^t \phi_k(\tau)\mathrm{d}\tau, \tag{108}$$

$$b(t) = b_0 + \int_0^t v_B(\tau)\mathrm{d}\tau = b_0 + \sum_{k=1}^{n} b_k \int_0^t \phi_k(\tau)\mathrm{d}\tau. \tag{109}$$

Substitution of (108-109) in the place of $a(t)$ and $b(t)$ in the above theory ables us to express the control of leaves with the help of "velocity parameters of leaves".

The limited velocity means restrictions of the form

$$|\sum_{k=1}^{n} a_k \phi_k(t)| \leq v_M,\ |\sum_{k=1}^{n} b_k \phi_k(t)| \leq v_M,\ t \in [0,T] \tag{110}$$

for the parameters $a_k,\ b_k,\ k = 1, ..., n$. The unidirectionality of e.g. A-leaf can be obtained by choosing the positive basis functions ϕ_k and demanding that $a_k \geq 0$. For steplike basis the restrictions (110) are easy to handle. With the same kind of modifications the limited acceleration of the leaves can be taken into account.

The other possibility to take into account the limitations of velocity (and acceleration) is to assume that the basis system ϕ_k for leaf trajectories $a(t),\ b(t)$ is (twice) differentiable. Then $v_A(t) = a'(t) = \sum_{k=1}^{n} a_k \phi_k'(t)$ and similarly for the B -leaf. For example, the limited velocity of A-leaf means the restriction $|\sum_{k=1}^{n} a_k \phi_k'(t)| \leq v_M$, for each $t \in [0,T]$.

8 Acknowledgements

This work was supported by TEKES (Technology Development Centre Finland) and Varian Medical Systems Finland, Espoo, Finland.

9 APPENDIX

Lemma 1 *Let $b_1 \leq a_1 \leq a_2 \leq b_2$ and let τ be a small positive number. Then*

$$\int_{b_1}^{b_2} e^{-(x-v)^2/\sigma^2} (\mathrm{erf}_\tau(a_2 - v) - \mathrm{erf}_\tau(a_1 - v))\mathrm{d}v$$
$$\approx \sqrt{\pi}\sigma(\mathrm{erf}_\rho(a_2 - x) - \mathrm{erf}_\rho(a_1 - x)) \tag{111}$$

where $\rho = \sqrt{\sigma^2 + \tau^2}$.

Proof. Since erf_τ approximates the Heaviside function when τ is small we find that

$$\begin{aligned}&\int_{b_1}^{b_2} e^{-(x-v)^2/\sigma^2}(\mathrm{erf}_\tau(a_2 - v) - \mathrm{erf}_\tau(a_1 - v))\mathrm{d}v \\ &\approx \int_{-\infty}^{\infty} e^{-(x-v)^2/\sigma^2}(\mathrm{erf}_\tau(a_2 - v) - \mathrm{erf}_\tau(a_1 - v))\mathrm{d}v. \end{aligned} \tag{112}$$

The approximation in (111) is due to the approximation (112) only. We have to show that the right hand side of (112) is equal to the right hand side of (111).

Denote

$$I(a_2) := \int_{-\infty}^{\infty} e^{-(x-v)^2/\sigma^2}\mathrm{erf}_\tau(a_2 - v)\mathrm{d}v \tag{113}$$

and

$$\begin{aligned} f_{x,\sigma}(v) &:= e^{-(x-v)^2/\sigma^2} \\ g_\tau(v) &:= \mathrm{erf}_\tau(v). \end{aligned}$$

Then we find that

$$I(a_2) = \int_{-\infty}^{\infty} f_{x,\sigma}(v) g_\tau(a_2 - v)\mathrm{d}v = \sqrt{2\pi}(f_{x,\sigma} * g_\tau)(a_2) \tag{114}$$

where $*$ refers to the convolution and where $\sqrt{2\pi}$ is a scaling factor. Hence we obtain for the corresponding Fourier transforms (in the sense of tempered distributions, see e.g. [21])

$$\hat{I} = \sqrt{2\pi}\hat{f}_{x,\sigma} \cdot \hat{g}_\tau. \tag{115}$$

From standard mathematical tables we see that the Fourier transform $\hat{f}_{x,\sigma}$ is

$$\hat{f}_{x,\sigma}(\xi) = \frac{\sigma}{\sqrt{2}} e^{-i\xi x - (\sigma\xi)^2/4} \tag{116}$$

Since $g'_\tau(v) = \frac{1}{\sqrt{\pi}\tau} e^{-v^2/\tau^2}$ and since $\widehat{g'_\tau}(\xi) = i\xi\hat{g}_\tau$ we find that

$$\hat{g}_\tau(\xi) = \frac{1}{\sqrt{2\pi}i\xi} e^{-(\tau\xi)^2/4} \tag{117}$$

for all $\xi \neq 0$. Combining (115, 116, 117) we get for $\xi \neq 0$

$$\begin{aligned} \hat{I} &= \sqrt{2\pi}\frac{\sigma}{\sqrt{2}} e^{-i\xi x - (\sigma\xi)^2/4} \frac{1}{\sqrt{2\pi}i\xi} e^{-(\tau\xi)^2/4} \\ &= \sqrt{\pi}\sigma e^{-i\xi x}\hat{g}_\rho = \sqrt{\pi}\sigma \widehat{g_\rho((\cdot) - x)} \end{aligned} \tag{118}$$

since $e^{-i\xi x}\hat{g}_\rho = \widehat{g_\rho((\cdot) - x)}$. In the second step we applied (117) replacing τ with ρ. The assertion follows from (118) by taking Fourier inverse transforms.

References

[1] T. Bortfeld, D.L. Kahler, T.J. Waldron and A.L. Boyer. X-ray field compensation with multileaf collimators. *Int. J. Radiat. Biol. Phys.* 28: 723–730, 1994

[2] C. Börgers. The radiation therapy planning problem. In C. Börgers and F. Natterer, editors, *Computational radiology and imaging: Therapy and diagnostic*. Springer, 1997

[3] Y. Censor, M.D. Altschuler and W.D. Powlis. On the use of Cimmino's simultaneous projections method for computing a solution of the inverse problem in radiation therapy treatment planning. *Inv. Prob.* 4: 607–623, 1988

[4] Y. Censor and S.A. Zenios. *Parallel optimization: theory, algorithms and applications.* UOP, 1997

[5] A. Gustafsson, B.K. Lind, R. Svensson and A. Brahme. Simultaneous optimization of dynamic multileaf collimation and scanning patterns of compensation filters using a generalized pencil beam algorithm. *Med. Phys.* 22: 1141–1156, 1994

[6] T. Holmes and T.R. Mackie. A comparison of three inverse treatment planning algorithms. *Phys. Med. Biol.* 39: 91–106, 1994

[7] R. Horst and H. Tuy *Global Optimization. Deterministic Approaches.* Springer, 1996

[8] D.H. Hristov and B.G. Fallone. An active set algorithm for treatment planning optimization. *Med. Phys.* 24: 1455–1464, 1997

[9] P. Kolmonen , J. Tervo and T. Lahtinen The use of Cimmino algorithm and continuous approximation for dose deposition kernel in the inverse problem of radiation treatment planning. *Phys.Med.Biol.* 43: 2539–2554, 1998

[10] C.L. Lawson and R.J. Hanson. *Solving Least Squares Problems.* SIAM Publications, 1995

[11] S. Lee, P.S. Cho, R.J. Marks and S. Oh. Conformal radiotherapy computation by the method of alternating projections onto convex sets. *Phys. Med. Biol.* 42: 1065–1086, 1997

[12] J. Löf, B.K. Lind and A. Brahme. An adaptive control algorithm for optimization of intensity modulated radiotherapy considering uncertainties in beam profiles, patient set-up and internal organ motion. *Phys. Med. Biol.* 43: 1605–1628, 1998

[13] J.D. Pinter. *Global Optimization in Action.* Kluwer Academic Publishers, 1996

[14] S.V. Spirou and C-S. Chui. Generation of arbitrary intensity profiles by combining the scanning beam with dynamic multileaf collimation. *Med. Phys.* 23: 1–8, 1996

[15] S.V. Spirou and C-S. Chui. A gradient inverse planning algorithm with dose-volume constraints. *Med.Phys.* 25: 321–333, 1998

[16] J. Stein, T. Bortfeld, B. Dörschel and W. Schlegel. Dynamic x-ray compensation for conformal radiotherapy by means of multileaf collimation. *Radiother.Oncol.* 32: 163–173, 1994

[17] R. Svensson, P. Källman and A. Brahme. Analytical solution for the dynamic control of multileaf collimators. *Phys. Med. Biol.* 39: 37–61, 1994

[18] J. Tervo and P. Kolmonen. Data fitting model for the kernel of integral operator from radiation therapy. *Mathl. Comput. Modelling* 28: 59–77, 1998

[19] J. Tervo, P. Kolmonen, M. Vauhkonen, L.M. Heikkinen and J.P. Kaipio. A finite element model of electron transport in radiation therapy and related inverse problem. *Inv. Probl.*, to apper, 1999

[20] J. Tervo, P. Kolmonen, T. Lyyra-Laitinen, J.D. Pinter and T. Lahtinen. An optimization-based approach to the multiple static technique in radiation therapy. *Report A/1999/4.* University of Kuopio, Department of Compute Science and Applied Mathematics, 1999

[21] F. Treves. *Topological vector spaces, distributions and kernels.* Academic Press, 1967

[22] P. Xia and L.J. Verhey. Multileaf collimator leaf sequencing algorithm for intensity modulated beams with multiple static segments. *Med. Phys.* 25: 1424–1434, 1998

[23] W. Ulmer and D. Harder. A triple Gaussian pencil beam model for photon radiations in treatment planning. *Z. Med. Phys.* 5: 25–30, 1995

[24] W. Ulmer and D. Harder. Application of a triple Gaussian pencil beam model for photon beam treatment planning. *Z. Med. Phys.* 6: 68–74, 1996

[25] X.H. Wang, R. Mohan, A. Jackson, S.A. Leibel, Z. Fuks and C.C. Ling. Optimization of intensity-modulated 3D conformal treament plans based on biological indices. *Radiother. Oncol.* 37: 140–152, 1995

[26] S. Webb. *The Physics of Three-Dimensional Radiation Therapy.* IOP Publishing, 1993

[27] S. Webb. *The Physics of Conformal Radiotherapy: Advances in Technology.* IOP Publishing, 1997

[28] S. Webb. Configuration options for intensity-modulated radiation therapy using multiple static fields shaped by a multileaf collimator. *Phys. Med. Biol.* 42: 595–602, 1998